Limiting factors in sub-10 nm scanning-electron-beam lithography

Bryan Cord,[a] Joel Yang, and Huigao Duan
Massachusetts Institute of Technology, Cambridge, Massachusetts 02139

David C. Joy
Oak Ridge National Laboratory, Oak Ridge, Tennessee 37831

Joseph Klingfus
Raith USA, Ronkonkoma, New York 11779

Karl K. Berggren
Massachusetts Institute of Technology, Cambridge Massachusetts

(Received 9 July 2009; accepted 28 September 2009; published 1 December 2009)

Achieving the highest possible resolution using scanning-electron-beam lithography (SEBL) has become an increasingly urgent problem in recent years, as advances in various nanotechnology applications [F. S. Bates and G. H. Fredrickson, Annu. Rev. Phys. Chem. **41**, 525 (1990); Black *et al.*, IBM J. Res. Dev. **51**, 605 (2007); Yang *et al.*, J. Chem. Phys. **116**, 5892 (2002)] have driven demand for feature sizes well into the sub-10 nm domain, close to the resolution limit of the current generation of SEBL processes. In this work, the authors have used a combination of calculation, modeling, and experiment to investigate the relative effects of resist contrast, beam scattering, secondary electron generation, system spot size, and metrology limitations on SEBL process resolution. In the process of investigating all of these effects, they have also successfully yielded dense structures with a pitch of 12 nm at voltages as low as 10 keV. © *2009 American Vacuum Society.* [DOI: 10.1116/1.3253603]

I. INTRODUCTION

Achieving the highest possible resolution using scanning-electron-beam lithography (SEBL) has become an increasingly urgent problem in recent years, as advances in various nanotechnology applications[1–3] have driven demand for feature sizes well into the sub-10 nm domain, close to the resolution limit of the current generation of SEBL processes. In this work, we have used a combination of calculation, modeling, and experiment to investigate the relative effects of resist contrast, beam scattering, secondary electron generation, system spot size, and metrology limitations on SEBL process resolution. Our work has shown that all of these factors affect resolution at sub-10 nm scales much less than previously thought, and that the current barrier to higher-resolution SEBL may be related to specific properties of the resists generally used for SEBL processing. In the process of investigating all of these effects, we have also successfully yielded dense structures with a pitch of 12 nm at voltages as low as 10 keV.

II. THEORETICAL RESOLUTION LIMIT

Most recent work on SEBL resolution enhancement has focused on increasing the contrast of the development process.[4–7] While this approach has been very successful thus far, our calculations show that, past a certain point, improved contrast will not result in improved resolution, and that the minimum achievable feature size will ultimately be limited by the point-spread function (PSF) of the exposing radiation, rather than the contrast of the development process.

To illustrate this, consider the idealized contrast curve and dense/isolated deposited energy profile shown in Fig. 1. We have assumed that the features here are single-pixel lines and that the point-spread function is finite and Gaussian, which results in a "blurring" of the dense features and an overall maximum dose in the dense region that is slightly higher than the maximum isolated dose. In order for both the dense and isolated structures in this pattern to yield, two criteria need to be met: the minimum dose of the dense features must be $\leq D_0$ and the maximum dose of the isolated features must be $\geq D_1$. In practice, of course, proximity-effect correction could be used to make the dense and isolated doses more uniform, but this simplified example illustrates the basic relationship between the PSF, contrast, and resolution; a pattern exposed with a narrow PSF can yield even with a low-contrast resist process, and a high-contrast resist process can successfully develop patterns exposed with a wider PSF.

To quantify this relationship, we assumed a one dimensional dose distribution made up of both a single Gaussian (isolated feature) and an infinite series of Gaussians at a given pitch (dense features). We then used this pattern to numerically determine the minimum pitch, as a fraction of the point-spread function, that would satisfy the yield criteria in Fig. 1 for a given contrast. The results of this calculation are plotted in Fig. 2.

Figure 2 clearly illustrates both the advantages and disadvantages of contrast enhancement. For hydrogen silsesquioxane (HSQ) resist, moving from standard tetra-methyl-

[a]Electronic mail: bcord@alum.mit.edu

 1071-1023/2009/27(6)/2616/6/$25.00 ©2009 American Vacuum Society

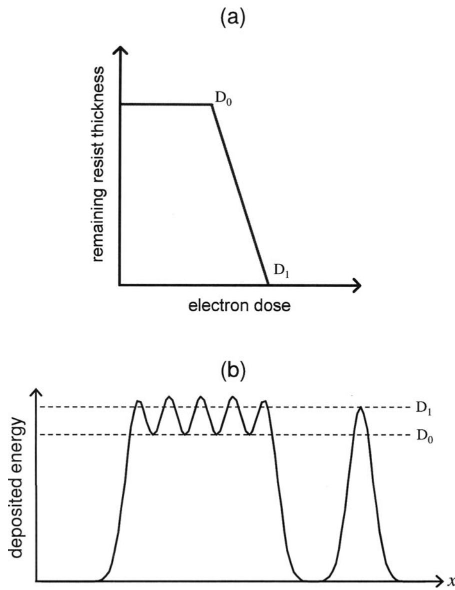

FIG. 1. (a) Schematic illustration of a resist contrast curve with the D_0 and D_1 doses labeled. (b) Deposited energy profile for a pattern consisting of both dense and isolated features, with the contrast requirements required for the pattern to yield superimposed. In order for the feature to yield, the top of the isolated feature must be $\geqslant D_1$ while the lowest point in the dense features must be $\leqslant D_0$.

ammonium-hydroxide (TMAH)-based development to the "salty" development process of Yang and Berggren results in a substantial gain in resolution.[7] Increasing the contrast past this point, however, will change the final resolution very little due to the asymptotic nature of the relationship; even with infinite contrast, the minimum yieldable pitch in a dense/isolated feature will be $\sim 1.01\times$ the full width at half maximum (FWHM) of the PSF. While this result essentially rules out any further effort to increase resist contrast, it also implies that the theoretical resolution limit of SEBL is much

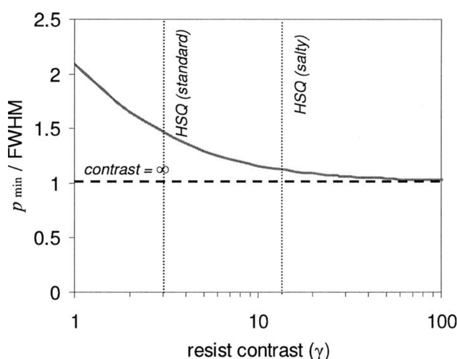

FIG. 2. Minimum pitch at which it is possible to yield both isolated and dense features (normalized to the FWHM of the point-spread function) as a function of resist contrast. Increasing resist contrast does, to a point, increase theoretical resolution, as illustrated by the difference between the standard development process for hydrogen silsesquioxane (HSQ) (a high-resolution negative electron-beam resist) and the salty process developed by Yang and Berggren, but the gains are asymptotic. Further increase in the contrast is unlikely to translate into substantially better resolution, and even with an infinite-contrast resist, resolution is limited to approximately the FWHM of the beam's point-spread function.

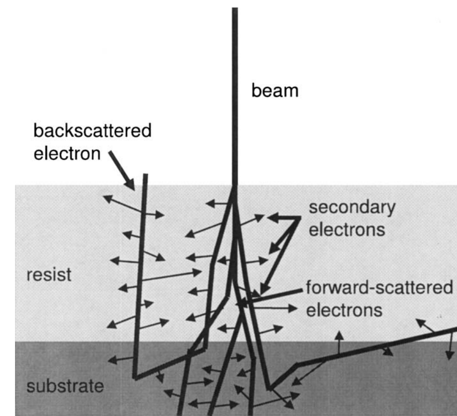

FIG. 3. Schematic illustration of the various processes that influence the point-spread function. An electron beam traveling through a resist film can interact with particles both elastically (producing forward scattering and beam broadening) and inelastically (producing secondary elections). Additionally, electrons can backscatter out of the substrate, although this effect can usually be ignored when performing resolution diagnostics on small, low-density features.

higher than previously thought; for example, when "salty development" is used to develop a pattern exposed in a SEBL system with a PSF on the order of 5 nm, it should at least in principle be possible to yield dense/isolated structures with a pitch of ~ 6 nm, i.e., 3-nm-wide lines and spaces! It should be mentioned again that this is an idealized calculation, but an empirical result even approaching this value would represent a major breakthrough.

III. THE POINT-SPREAD FUNCTION

Having established that the PSF is in principle the primary resolution limiter in our process, the obvious question is "what sets the PSF width and what can we do about it?" In the previous paragraph we assumed that the PSF was approximately equal to the tool beam diameter, but there are two other contributors to the PSF width to consider: primary beam scattering and secondary electrons, as illustrated in Fig. 3.

Primary beam scattering occurs when electrons in the beam elastically collide with atomic nuclei in the material and their trajectory is subsequently altered.[8] It is commonly described as two subprocesses: *forward scattering* causes broadening of the incident beam through collisions and *backscattering* causes scattering back out of the substrate and through the resist. Backscattering, which causes beam spreading over length scales of several microns, is not directly relevant to our discussion of resolution at the nanoscale (for the structures being studied here, it can be treated as a small, constant dose offset and thus can be safely ignored), so we will limit our discussion to forward scattering here.

The extent of the forward scattering is primarily determined by the resist thickness and the beam energy. Thicker resist will induce more broadening, as the beam has more distance to travel once deflected, while higher beam energy will reduce scattering by reducing the trajectory change each

electron incurs in a collision. As a result, the standard way to eliminate forward scattering is to use thin resist and/or high beam energies.

While forward scattering is caused by elastic collisions between electrons in the incident beam and particles in the material, it is also possible for inelastic collisions to occur, transferring energy to particles in the resist and occasionally freeing a valence electron. These secondary electrons, with energies ranging from a few eV to (with low probability) nearly half the incident beam energy, typically travel normal to the primary beam and can deposit a substantial amount of energy in the resist.[9] The dependence of the secondary electron range on resist thickness and beam energy is not well known, but evidence suggests that their range is relatively independent of both parameters.[9,10] Since the initial diameter of the beam (commonly referred to as the "spot size") also has no dependence on the resist thickness or, at least in principle, the beam energy, the spot size and secondary electrons can be thought of as a constant offset to the final PSF width, independent of the beam energy and resist system.

In order to calculate the relative effects of the initial beam diameter, forward scattering, and secondary electrons on the final PSF width, we used a Monte Carlo simulation. The code was based on the single-scattering model developed by Joy.[11] The screened Rutherford cross section was used to characterize elastic collisions and the Evans cross section was used for inelastic collisions; data suggest that other possible inelastic cross sections would give very similar results.[12] While most published Monte Carlo simulations that include secondary electrons have simply calculated their ranges in the resist, our program instead tracked the energy deposited in the resist film via Bethe slowing by each primary and secondary electron, then generated a two dimensional representation of the spatial deposited energy profile, the FWHM of which was then measured. This treatment of the electron behavior is more relevant to the discussion of resist exposure than electron-range calculations would be. We ran the simulation for HSQ thicknesses ranging from 25 to 250 nm and incident beam energies ranging from 10 to 100 keV, using an incident Gaussian beam with a FWHM of 5 nm, to simulate conditions in our RAITH150 system. The simulation results are plotted in Fig. 4, with curve fits to accentuate each data set.

For low primary beam energies and thick resists, forward scattering dominates the point-spread function and produces the expected broadening. However, past a certain beam energy for a given resist thickness, forward scattering is small enough so that it ceases to be an issue, and the width of the PSF is approximately equal to the width of the incident beam. Interestingly, secondary electrons do not appear to significantly affect the PSF here; although their yields and ranges correspond with previously published results, the energy they actually contribute to the PSF is dwarfed by the contribution of the primaries. As this contradicts much of the conventional wisdom in the literature,[9,10] it should be noted that the simulation is somewhat simplistic, neglecting effects such as secondary cascades (secondary electrons producing

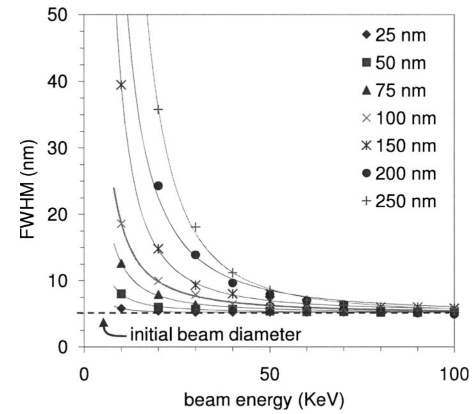

FIG. 4. Monte Carlo measurements of the deposited energy distribution point-spread function at the base of HSQ layers of varying thickness, as a function of beam energy. The initial beam profile is assumed to be Gaussian with a FWHM of 5 nm here. For low energies and/or thick resists, forward scattering substantially broadens the PSF, but as the beam energy is increased and/or the thickness is reduced, the FWHM collapses to nearly the initial beam diameter. Secondary electrons, interestingly, seem to have little to no effect on the PSF width, a result which contradicts conventional wisdom.

secondaries of their own) and chemical changes induced in the resist during exposure. It is possible that more a more thorough model would show a larger energy contribution from secondaries.

As Fig. 5 illustrates, for resist thicknesses below a certain "critical thickness," the FWHM of the deposited energy profile is essentially identical to the FWHM of the incident beam, while for thicknesses above the critical thickness, the FWHM will be broadened by forward scattering in the resist. This critical thickness plot was calculated graphically from the data in Fig. 4 by finding the energy at which the FWHM for a given resist thickness was <1 nm greater than the initial beam diameter, indicating that forward scattering had

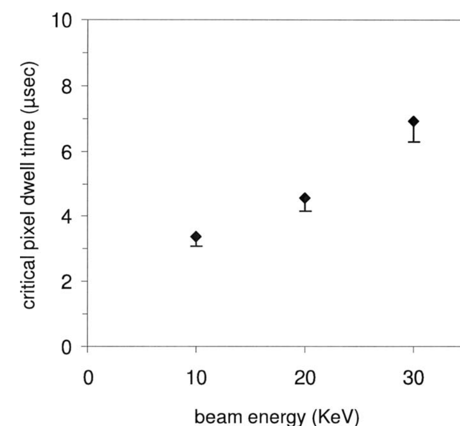

FIG. 5. Critical thickness of resist as a function of beam energy, as extracted from the data in Fig. 4 by taking the approximate energy at which the PSF was <1 nm greater than the initial beam diameter for each given resist thickness (the solid line is a generic fit function to serve as a visual aid). At resist thicknesses above the critical thickness, forward scattering limits resolution, whereas below the critical thickness the only resolution limiter (when considering only the exposure process, at least) is the beam diameter, which is at least theoretically energy independent.

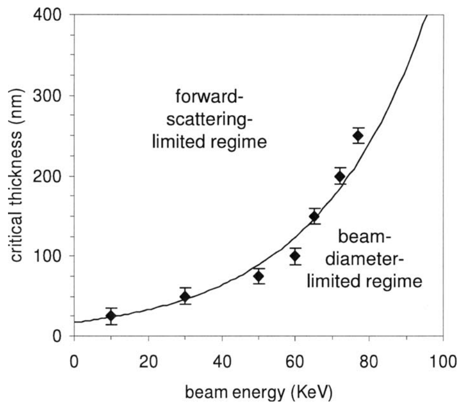

FIG. 6. Critical pixel dwell time (the minimum time the beam needs to dwell on a single pixel in order to expose it) as a function of beam energy, calculated using the system beam current and minimum dose required for a small (no significant backscattering effects) feature to fully develop at a given acceleration voltage. The error bars here represent the uncertainty in deriving a critical dose from a single element in a dose array. Even taking into account the lower beam current at 10 keV (which we have done here), the critical dwell time is nearly a factor of 2 lower than it is at 30 keV, resulting in a nearly two times increase in throughput when writing at 10 keV.

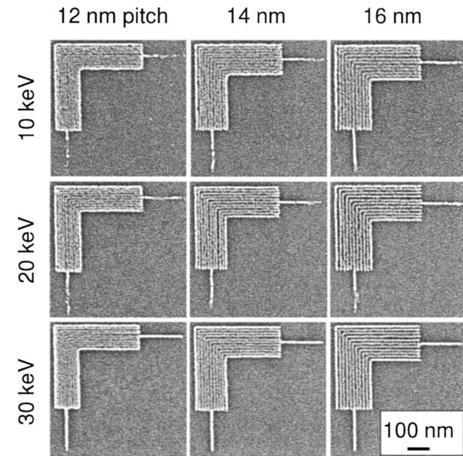

FIG. 7. Scanning electron micrographs of nested-L structures with pitches ranging from 12 (the smallest yielded at any voltage) to 16 nm, exposed at 10, 20, and 30 keV in 25 nm of HSQ on a Si substrate. The resist was developed for 4 min using 1% NaOH/4% NaCl, and the developed features were coated with 2 nm of Au–Pd prior to imaging. While there is some resolution degradation at lower acceleration voltages for the smaller pitches, it is minimal and, at 16 nm and above, almost completely absent.

ceased to be a major issue at this energy, then plotting the results as critical thickness versus energy rather than critical energy versus thickness. Since the beam diameter is, in principle, independent of beam energy in a good SEBL system (we will see later that this is not exactly true in practice), this means that *beam energy is irrelevant as long as it is high enough to keep critical thickness above the resist thickness!* This means, for example, that it should be possible to get near-identical resolution in a 50 nm HSQ stack using a 100 keV SEBL system and an inexpensive 30 keV system (assuming the beam diameters are similar). This conclusion contradicts the conventional wisdom that high beam energies are necessary for high resolution and indicates that, for our process parameters (25-nm-thick resist, 10–30 keV exposure energy), beam broadening is not a serious issue.

An incidental advantage to patterning at low energies is an increase in throughput. Low-energy electrons deposit energy in resist much more efficiently than high-energy electrons, meaning it takes fewer electrons to expose a pattern at low beam energies. This advantage is somewhat offset by the fact that beam current tends to be proportional to beam energy in most systems but, at least on the RAITH150, there is still a substantial net gain in exposure speed, as Fig. 6 illustrates.

IV. EXPERIMENTAL RESULTS

In order to verify the resolution limit calculation in Sec. I, we experimentally tested the minimum feature sizes that could be achieved when patterning dense/isolated structures and used the results to estimate the PSF of the exposure process. To do this experiment, HSQ was spin coated onto a standard silicon substrate to a thickness of approximately 25 nm, which should be below the critical thickness discussed earlier at the beam energies being used and allow us to neglect scattering. The resist was then exposed to a pattern consisting of "nested-L" resolution test structures at various pitches and doses in MIT's RAITH150 SEBL system, which has a rated beam diameter of 3–5 nm. Write voltages of 10, 20, and 30 keV were used, in order to test the beam-energy independence that our simulations show should be present when the resist is thinner than the critical thickness. All samples were developed in an aqueous solution of 1% NaOH/4% NaCl (salty development) for 4 min at 24 °C, rinsed under a continuous de-ionized water flow for 60 s, quickly rinsed with isopropanol to remove residual water, and blow dried with a nitrogen gun. The developed samples were then coated with 2 nm of Au–Pd and imaged using the RAITH150. The best results from these experiments are shown in Fig. 7.

As Fig. 7 illustrates, the smallest pitch at which we were able to observe any modulation in dense/isolated structures was approximately 12 nm. Since 25 nm is below the critical thickness in both the 20 and 30 keV cases, and approximately equal to it in the 10 keV case, the results at all three write voltages are similar, verifying our earlier conclusion that beam energy is irrelevant if the resist is thin enough (similar results were also obtained with resist as thin as 10 nm). While yielding 6 nm lines and spaces is certainly still respectable, the result of our resolution limit calculation in Sec. III suggested that yielding structures almost a factor of 2 smaller than this (3 nm lines and spaces) in thin resist should be possible in our system, which has a rated beam diameter of 3–5 nm. Since this is nearly a factor of 2 smaller than what we were actually able to achieve, and beam broadening in the resist has been ruled out as a resolution limiter, there appears to be a limiting factor in our process that we have not yet taken into account.

V. ANALYSIS

Having established that the PSF in our process should be approximately identical to the initial beam diameter, we decided to directly measure the beam diameter to verify that it was within the specifications provided by the tool vendor, and not being broadened by some external factor, such as system noise or vibrations.

Our method for measuring the beam diameter was a variation in the standard ASTM procedure for characterizing scanning electron microscopes.[13] Our measurement sample was a standard gold-on-carbon scanning electron microscopy (SEM) characterization sample purchased from Ted Pella, Inc. Our method hinged on the assumption that a Gaussian-profile beam scanned in a line over an edge approximated as a step function will produce a SEM signal that is a convolution of the two shapes. In principle, the width of the Gaussian beam can then be deconvolved from the linescan produced by the SEM. We recognize that in practice the signal produced by the SEM will not actually look like a convolution of a Gaussian and step function, as this approximation ignores the "bump" in the signal created by increased secondary electron yield at the feature edge. This effect should be able to be safely neglected, however, by using the signal level far away from the feature edge as the baseline for the signal maximum.

In order to do the measurement, a high-magnification image was taken of the test sample, the brightness and contrast were adjusted to ensure that the image was not saturated, and three linescans each were taken over edges in the x and y directions. This procedure was repeated for 30 images for each voltage measured, in order to minimize random errors originating from irregular edge shapes and other sources. The linescans were processed with a moving-average filter to remove noise, then measured by taking the distance between the points of 80% maximum value (the maximum value being measured far from the edge of the feature, as previously mentioned) and 20% maximum value on the slope, which was calculated to correspond to ~71% of the beam's FWHM. The results of these measurements at acceleration voltages of 1, 5, 10, and 20 keV are plotted in Fig. 8. The 30 keV diameter, unfortunately, could not be measured because the in-lens secondary electron detector in the RAITH150 does not work at this voltage, making imaging effectively impossible. Still, the beam diameter at 30 keV can be reasonably extrapolated from the data we were able to obtain.

At the 10, 20, and 30 keV energies of interest, these results are within the specification of the RAITH150. Based on these data, beam diameter does not appear to be a serious limiting factor in our resolution. However, superior resolution (9 nm pitch) obtained on Raith's prototype RAITH150 Mark II system (which differs from MIT's RAITH150 primarily in having a spot size that is 2–3 nm smaller) suggests that beam diameter does, in fact, affect minimum feature size, even when the beam is much narrower than the minimum feature size.[14]

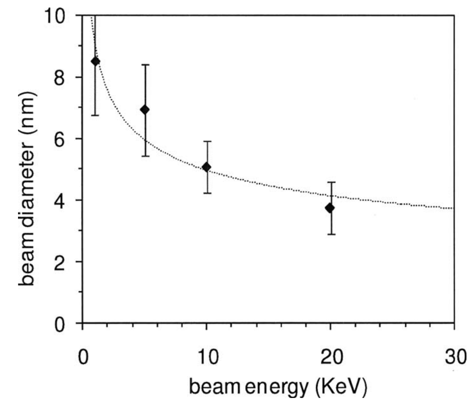

FIG. 8. Beam diameter as a function of beam energy as measured in the MIT RAITH150 system. Each data point represents 90 linescans in the x direction (the data from the y direction scans were identical to within the margin of error). Within the voltage range being used for lithograph (10–30 keV), the beam diameter appears to be close to its 3–5 nm specification. This suggests that beam diameter is not the limiting factor in our resolution.

Another possible reason for the discrepancy between our theoretical and observed resolution is that the *imaging* resolution of the RAITH150 may be lower than its *lithographic* resolution. When the RAITH150 is writing patterns, the beam dwell time on a single pixel is typically on the order of 1 μs. At these beam speeds, the bandwidth of environmental noise capable of distorting or blurring patterns is on the order of 100 kHz–1 MHz or larger.

Imaging is another issue entirely. When the RAITH150 is being used for imaging, the system is scanning the beam comparatively slowly and is consequently vulnerable to electronic and acoustic noise in the 1 Hz–1 kHz range, as well as the higher frequencies mentioned earlier. These additional low-frequency vibrations can be extremely difficult to compensate for, and the result can be an imaging resolution that is limited by system noise, rather than beam diameter. If this is, in fact, the case, our RAITH150 may be fabricating structures that it cannot successfully image.

In order to answer the imaging-versus-lithographic resolution question definitively, we fabricated several samples on 50-nm-thick SiN membranes and imaged them using transmission electron microscopy (TEM). The resolution of TEM is typically on the order of angstroms, so even the smallest structures we were able to fabricate using SEBL should be easily visible. All imaging was performed using a JEOL 2010 TEM, with an operating voltage of 200 keV. Figure 9 shows the best lithographic resolution observed using TEM analysis thus far.

As the smallest features we were able to image using a TEM were approximately the size of our best SEM results (6 nm structures, corresponding to a pitch of ~12 nm), we concluded that issues with SEM imaging, while possibly accounting for a nanometer or two of "lost resolution," were not the reason our minimum achievable real-world resolution was so much lower than theoretical predictions.

While both have some detrimental effect on resolution, the contributions of the beam diameter and imaging limitations are not sufficient to account for the large discrepancy between our observed and calculated maximum resolutions.

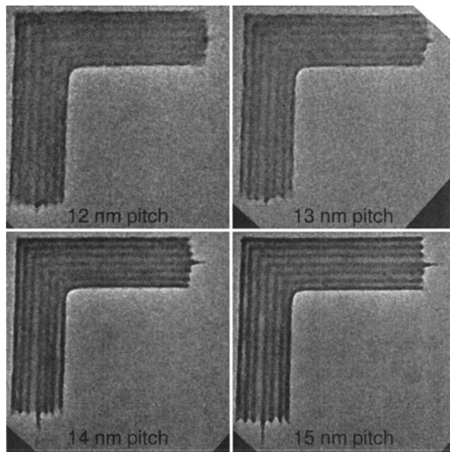

FIG. 9. Transmission electron micrographs of several 50-nm-thick HSQ nested-L structures fabricated on a 50-nm-thick SiN membrane. While the imaging resolution is much higher than on a typical SEM (evidenced by the visible line-edge roughness, footing around the lines, and texture on the membrane itself), the observed lithographic resolution is approximately equal to the SEM results in Fig. 3, with 12 nm being the lowest pitch at which any modulation was visible. This result suggests that limitations in our SEM imaging are not the reason our observed maximum resolution is so much lower than the calculated theoretical maximum.

As a result, we were forced to look beyond the exposure process for an explanation. HSQ being the resist used in the vast majority of our resolution experiments, the logical next step was to investigate the development mechanics of HSQ. Unlike PMMA and most other resists, HSQ has a highly nonlinear development rate, as demonstrated by Yang *et al.*[14] The reason for this self-limiting behavior is unknown, but we hypothesize that it is due to a combination of negative charge buildup on the resist surface during development and/or cross-linked material in the developing resist. When combined with the fact that mass transfer issues are known to slow down development rates for small, deep features (such as the gaps in our dense HSQ gratings) by limiting the flow of developer into the reaction site and reaction product out of the reaction site,[15] it seems plausible that, in gaps below a certain threshold width, undeveloped HSQ cannot dissolve quickly enough to create a gap visible to SEM/TEM imaging before the reaction self-limits. If this is the case, the final resolution of HSQ-based lithography is limited by the resist itself, not the exposure tool. Quantifying this effect is difficult, however, and more detailed modeling and experimental evidence are needed before it can be considered more than a working hypothesis.

VI. CONCLUSION

While we have not decisively found the limiting factor in SEBL resolution, we have presented evidence that resist contrast, beam scattering, secondary electrons, and initial beam diameter have only slight, if any, effect on final resolution in certain situations, and that sub-10 nm patterning of simultaneous dense and isolated features is possible even at exposure energies as low as 10 keV. The primary factor limiting resolution in HSQ processes at this point is likely the development behavior of the resist, although quite a bit of work remains in order to fully quantify and understand this behavior. Since our choice of HSQ as a resist for our characterization work was essentially a matter of convenience (unlike PMMA, it can be imaged directly in a SEM and the developed structures are very sturdy), finding a new material to work with that has the benefits of HSQ but with improved development behavior may be the path to achieving further resolution improvement in SEBL.

[1]F. S. Bates and G. H. Fredrickson, Annu. Rev. Phys. Chem. **41**, 525 (1990).
[2]C. T. Black, R. Ruiz, G. Breyta, J. Y. Cheng, M. E. Colburn, K. W. Guarini, H. C. Kim, and Y. Zhang, IBM J. Res. Dev. **51**, 605 (2007).
[3]J. Yang, Z. Sun, W. Jiang, and L. An, J. Chem. Phys. **116**, 5892 (2002).
[4]G. H. Bernstein, D. A. Hill, and W. Liu, J. Appl. Phys. **71**, 4066 (1992).
[5]B. Cord, J. Lutkenhaus, and K. K. Berggren, J. Vac. Sci. Technol. B **25**, 2013 (2008).
[6]L. E. Ocola and A. Stein, J. Vac. Sci. Technol. B **24**, 3061 (2006).
[7]J. K. W. Yang and K. K. Berggren, J. Vac. Sci. Technol. B **25**, 2025 (2007).
[8]R. J. Hawryluk, H. I. Smith, and A. M. Hawryluk, J. Appl. Phys. **45**, 2551 (1974).
[9]D. C. Joy, Microelectron. Eng. **1**, 103 (1983).
[10]A. N. Broers, IBM J. Res. Dev. **32**, 502 (1988).
[11]D. C. Joy, *Monte Carlo Modeling for Electron Microscopy and Microanalysis* (Oxford University Press, New York, 1995).
[12]K. Murata, D. F. Kyser, and C. H. Ting, J. Appl. Phys. **52**, 4396 (1980).
[13]ASTM E986-04 (2004), "Standard Practice for Scanning Electron Microscope Beam Size Characterization," *Annual Book of ASTM Standards*, ASTM International, West Conshohocken, PA, 2004.
[14]J. K. W. Yang, B. Cord, J. Klingfus, S. Nam, K. Kim, M. J. Rooks, and K. K. Berggren, J. Vac. Sci. Technol. B (to be published).
[15]B. Cord, C. Dames, J. Aumentado, and K. K. Berggren, J. Vac. Sci. Technol. B **24**, 3139 (2006).